Separation of Hydrogen Sulfide from Butane Gas Mixture by Zeolite 13X

Garshasbi, Vahid; Jahangiri, Mansour*[+]

Faculty of Chemical, Petroleum and Gas Eng., Semnan University, Semnan, I.R. IRAN

Anbia, Mansoor

Research Laboratory of Nanoporous Materials, Faculty of Chemistry,
Iran University of Science and Technology, Tehran I.R. IRAN

ABSTRACT: *The Zeolitic adsorbent is successfully synthesized by natural Iranian kaolin to the separation of hydrogen sulfide from a gas mixture. In this work, zeolite 13X from modified natural Iranian kaolin at 65 °C for 72 h at various concentrations of caustic soda solution was synthesized using a metakaolinization process at 900 °C for 2h. By Taguchi's experimental design, the best duration and temperature of crystallization were 72 h and 65 °C. Prepared zeolite 13X was characterized using X-Ray Diffraction (XRD), Fourier Transforms InfraRed (FT-IR) spectroscopy, Scanning Electron Microscopy (SEM), and N_2 adsorption-desorption methods. In addition, the adsorption capacity of zeolite 13X for 310 ppm of hydrogen sulfide mixed with hydrocarbon gas-like butane was investigated using a volumetric method by two different detectors and different temperatures. After the adsorption process, the amount of H_2S in output gas was about 108 ppm and this confirms approximately more than 65% adsorption at 25 bar and 298K. The results are in good agreement with the experimental results.*

KEYWORDS: *Butane; Hydrogen sulfide; Hydrothermal synthesis; Zeolite 13X.*

INTRODUCTION

Zeolites are nanoporous inorganic materials for various important applications in catalysis, ion exchange, and separations [1-6]. A zeolite material is hydrated aluminosilicate compound that is prepared from tetrahedral alumina (AlO_4^{5-}) and silica (SiO_4^{4-}) through interlinkage of oxygen atoms [2-4]. The zeolites are usually synthesized from different sources of silica and alumina by hydrothermal treatment. To reduce the cost of synthetic zeolites, various sources for silica and alumina such as bentonite, lithium slag, high silicon fly ash, paper sludge, oil shale ash, coal fly ash, waste porcelain and kaolinite have been employed [7-14]. Kaolinite, $Al_2Si_2O_5(OH)_4$, is a mineral clay that consists of silica and alumina. For the synthesis of zeolite 13X from kaolinite, the amount of Al may be decreased or Si increased [15] with Si/Al values of above 1.5.

Zeolites adsorbents of 4A, 5A , and 13X may be used in the decontaminating process of low partial pressures of recovered components and high adsorption capacity for temperatures (up to 100 ºC) [16-17]. They tend to adsorb smaller molecules because of the uniform diameters of pore entrances [18-19]. So, in comparison to the other adsorbents like magnesium silicate, silica gel, activated charcoal, and MOFs (Metal-Organic Frameworks),

***** *To whom correspondence should be addressed.*
+ *E-mail: mjahangiri@semnan.ac.ir*
1021-9986/2022/11/3706-3717 12/$/6.02

they have the largest adsorption capacity for undesirable components [20].

Hydrogen sulfide (H_2S) is one of the major problems for most of the energy industries such as liquefied petroleum gas, natural gas, fuel cells, and transportation gases like diesel, gasoline, and jet fuels [21-23]. Hydrogen sulfide is toxic, colorless, corrosive, explosive, and soluble in hydrocarbons with an extremely rotten egg odor gas that tends to rapidly saturate the human olfactory system. Since 600 ppm rapidly provokes respiratory disturbance and leads to death, hence plant personnel and operators are at risk [24]. The corrosive effect of H_2S causes a lot of problems to equipment, pipelines, and downstream processes and causes huge economic losses, especially in the oil and gas industry. Therefore, controlling or removing hydrogen sulfide and other sulfur compounds to safe levels is necessary for the hydrocarbon processing industry [25]. It may be used traditional methods such as amine and sorbent treatment [26] to remove H_2S contamination from hydrocarbon streams. For trace amounts of hydrogen sulfide and high energy demand, amine treating is not a suitable method. So, in this case, sorbent materials such as zeolites are useful [27-29]. The physical adsorption properties of this group make it a downstream gas polishing treatment for the removal of trace amounts of sulfur compounds, H_2O, and CO_2, [30].

Because of zeolite application in industry and synthesis of it by cheap and available materials, in this work, we have synthesized the 13X zeolite from modified natural Iranian kaolin by hydrothermal treatment. The effect of NaOH concentration (1.0, 1.5, 2.0, 2.5, 3.0, 3.5, and 4M NaOH) was investigated, and synthesized products were characterized by X-Ray Diffraction (XRD), Fourier Transforms InfraRed (FT-IR), and Scanning Electron Microscopy (SEM), and N_2 adsorption-desorption methods. Finally, the selective adsorption of trace amounts of hydrogen sulfide from a gas mixture of butane by zeolite 13X will be investigated.

EXPERIMENTAL SECTION

Raw material

The natural kaolin (a source of silica and alumina) from Iranian sources was used for the present study. This kaolin had a high amount of SiO_2 and a low amount of Al_2O_3, so we modified it by acidizing to obtain convenient kaolin for the synthesis of 13X zeolite. Table 1 shows the properties of raw kaolin and modified kaolin. Metakaolin was obtained by calcining kaolin in a muffle furnace at 900 ˚C for 2h.

Table 1: Properties of natural kaolin before and after modification.

composition	Content (%)	
	kaolin	Modified kaolin
SiO_2	74.98	56.40
Al_2O_3	17.42	31.68
Fe_2O_3	0.54	0.26
TiO_2	0.96	0.28
CaO	1.62	0.65
MgO	0.27	0.24
Na_2O_3	1.04	0.31
K_2O	0.03	0.03
P_2O_5	0.12	0.11
L.O.I	3.02	10.04

Synthesis process

Different concentrations of caustic soda solutions of 1.0, 1.5, 2.0, 2.5, 3.0, 3.5, and 4 M were separately mixed with metakaolins. The samples were homogenized at room temperature for 20 min and then the reaction mixtures were distributed in an autoclave. The autoclave was kept in a conventional air oven at 65˚C for 72h at autogenous pressure. The product was washed with deionized water to reach a pH of 9 and then dried at 90˚C for 12h.

Characterization

The chemical composition of kaolin was determined by Bruker S4 wavelength Dispersive X-Ray Fluorescence Spectrometer (WDXRFS), with an Rh X-ray tube. The X-Ray powder Diffraction (XRD) patterns were recorded on a Philips PW1140/90 diffractometer using Cu-Kα target (40 kV, 25 mA) at the scan rate of 2^0/min and 2θ angles ranging from 5^0 to 80^0 with a step size of 0.02^0.

Infrared transmission spectra of the samples were made by the KBr wafer technique. The spectra were recorded on a Fourier transform infrared spectrometer system 2000 FT-IR (Perkin-Elmer). Morphological features of the sample surface were obtained by SEM images on VEGA3TESCAN.

Taguchi experimental design

The Design of Experiments (DOE) is developing a scheme of experiments in different conditions. Taguchi experimental

Table 2: Experimental variables and their levels.

Factor number	Parameter	Level 1	Level 2	Level 3
1	Relative alkalinity(Na_2O/ Al_2O_3) of the reaction mixture	4.5	5.5	6.5
2	SiO_2/Al_2O_3 ratio of the reaction mixture	2.5	3.5	4.5
3	The temperature of crystallization T(°C)	55	65	75
4	Duration of crystallization t(h)	24	48	72

Table 3: Taguchi L9 orthogonal array.

Run	Experiment condition			
	Na_2O/ Al_2O_3	SiO_2/Al_2O_3	Temperature (ºC)	time (h)
1	4.5	2.5	55	24
2	4.5	3.5	65	48
3	4.5	4.5	75	72
4	5.5	2.5	75	72
5	5.5	3.5	55	24
6	5.5	4.5	65	48
7	6.5	2.5	65	48
8	6.5	3.5	55	72
9	6.5	4.5	75	24

design is a well-known powerful and efficient tool for multifactor process optimization. Qualitek-4 software was utilized to design the experiments Taguchi approach. The capability of this software is the use of L_4 to L_{64} orthogonal arrays [31]. The impact of four factors and each factor in three levels, on the synthesis of zeolite 13X, was studied. Experimental variables and their levels are presented in Table 2 and Table 3 shows the nine induced experiments from Taguchi orthogonal design and their conditions.

Thermodynamic studies

The heat of adsorption, standard entropy, and standard free energy of the adsorption process was calculated according to the following relationships [2-6]:

$$\Delta G^0_{ads} = -RT \ln k \quad (1)$$

$$\ln k = \frac{\Delta S^0_{ads}}{R} - \frac{\Delta H^0_{ads}}{RT} \quad (2)$$

$$k = \frac{q_m}{q^b_e} \quad (3)$$

Where ΔG^0_{ads} (J/mol) is changes in standard Gibbs free energy, R $(J/mol\,K)$ is gas constant (8.314 J/mol K, k (g/mol) is the Langmuir equilibrium constant, T is the temperature in K, ΔH^0_{ads}(J/mol) change in standard enthalpy and ΔS^0_{ads} (J/mol K) change in standard entropy. Plotting of lnk versus 1/T gives a straight line with slope and intercept equal to ΔH^0_{ads} and ΔS^0_{ads}, respectively.

Gas adsorption measurement

We used the volumetric method to investigate the adsorption capacity of zeolite 13X for hydrogen sulfide (Fig. 1). This method for these gas uptake measurements is extensively adopted because of its low cost, simplicity, and easy assemblage [32-34]. At first, 1 g of sample was loaded in the adsorption reactor (high-pressure vessel) and attached to the system. Then the system was carefully checked to ensure all connections have no leakage and the existing gas inside the system was swept out with the inert Helium gas flow. For degassing the system, we opened the valves 5, 6, 7, 9 and closed other valves, then, turned on the vacuum pump and the system was vacuumed with the heating temperature of 523 K for 2 h. After degassing, the system was cooled to ambient temperature. The gas adsorption process was started by opening valves 3, 4, 5,

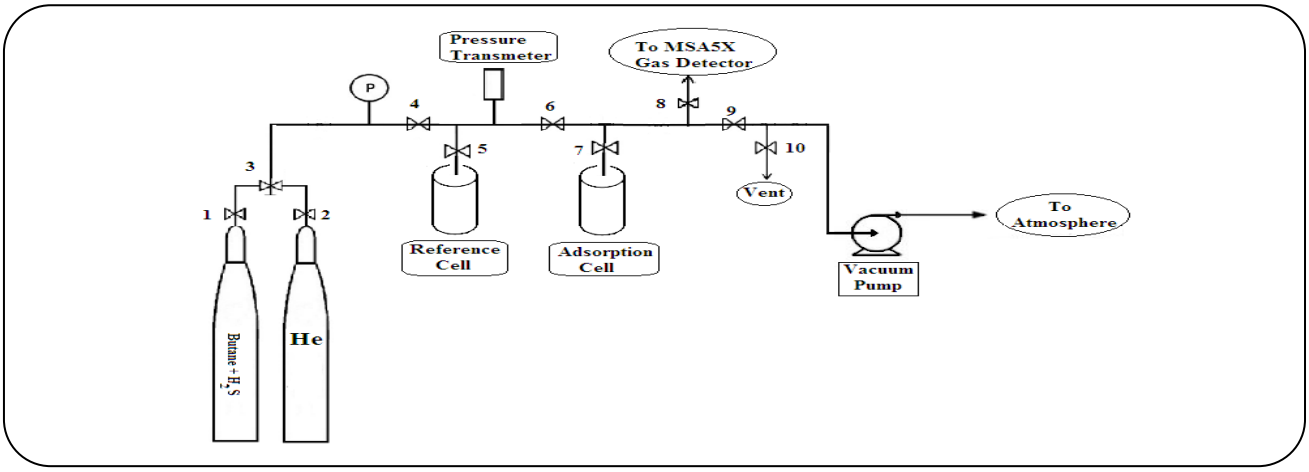

Fig. 1: Schematic flow chart of volumetric set up for gas adsorption test.

6, 7 and closing all other valves. Therefore the gaseous mixture (butane 99.99% and hydrogen sulfide 310 ppm) was introduced into the adsorption unit for H_2S adsorption measurements. An MSA5X gas detector was attached to the adsorption setup after the adsorption reactor to show the amount of H_2S in output gas. Therefore, the amount adsorbed by zeolite 13X can be calculated. To verify this result, a Gastec tube detector (4H, Japan) was used to monitor H_2S concentration for a second time.

RESULTS AND DISCUSSION

Characterization of adsorbent

From Table 1, it is observed that the main constituents of the natural kaolin were silica (74.98%) and alumina (17.42%). After modification, these percentages were silica (56.40%) and alumina (31.68%). Fig. 2 shows the XRD pattern of metakaolin and natural kaolin. Kaolinite is identified by its characteristic X-ray diffraction peaks at 12.30˚ and 24.60˚2θ that have been reported earlier [35].

The XRD pattern of metakaolin obtained by heating natural kaolin for 2h at 900˚C resembled others, except for the peaks due to admixed impurities. XRD pattern after heating shows a significant change in comparison to the untreated kaolin pattern. The highest diffraction peaks are very common in metakaolin amorphous structure that corresponds to the presence of quartz.

The XRD pattern of different products that are synthesized from different concentrations of NaOH is shown in Fig. 3. The formation of synthesized zeolite 13X in the products was detected, by comparing its d-values with d-values of the commercial zeolite 13X sample. The characteristic peaks of zeolite 13X are the most important

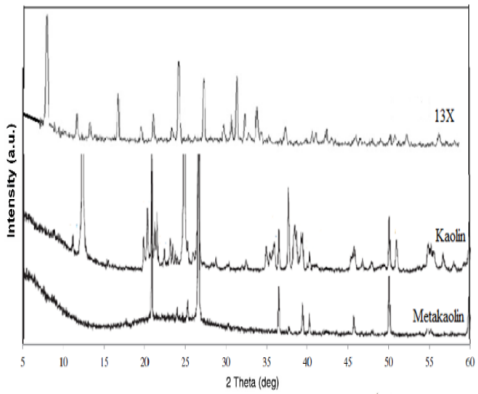

Fig. 2: XRD pattern of kaolin, metakaolin, and commercial zeolite 13X (from ref. [2]).

change observed in the XRD patterns. The synthesized products matched the characteristic peaks of zeolite 13X at 2θ values of 6.12˚, 10.00 ˚, 11.73 ˚ , 15.43 ˚,18.42 ˚,20.07 ˚,23.31 ˚,26.65 ˚,29.21 ˚,30.30 ˚,30.94 ˚,31.98 ˚,33.59 ˚ and 37.34 ˚. Fig. 3a, and 3b illustrate the XRD pattern of the product which was obtained from the sample with 1.0 M, 1.5 M, and 2.0 M NaOH solution that has a significant amount of metakaolin (amorphous) observed. With increasing NaOH concentration the results indicated that the synthesized zeolite products obtained from 2.5–4.0 M NaOH concentrations contain zeolite 13X as the major constituent phase.

Fig. 4 illustrates the IR spectra of different synthesized samples of zeolite 13X by reacted kaoline and commercial zeolite 13X. Spectrum a in Fig. 4 shows the broadband of metakaolin in the range from about 920 cm^{-1} to about 670 cm^{-1} and is assigned to Al-O bonds in Al_2O_3. During the

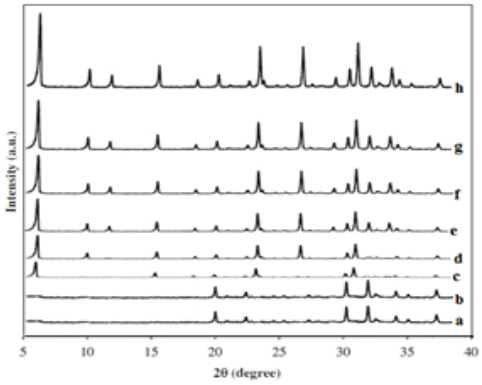

Fig. 3: XRD pattern of zeolite 13X and associated phases obtained by hydrothermal synthesis: (a) 1.0 M NaOH, (b) 1.5 M NaOH, (c) 2.0 M NaOH, (d) 2.5 M NaOH, (e) 3.0 M NaOH, (f) 3.5 M NaOH, (g) 4.0 M NaOH, and (h) commercial zeolite 13X.

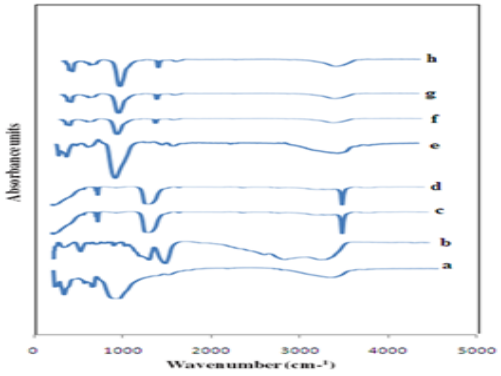

Fig.4: FTIR spectra of zeolite 13X and associated phases obtained by hydrothermal synthesis: (a) unreacted metakaolin, (b) 1.0 MNaOH, (c) 1.5 M NaOH, (d) 2.0 M NaOH, (e) 2.5 M NaOH, (f) 3.0 M NaOH, (g) 3.5 M NaOH, (h) 4.0 M NaOH.

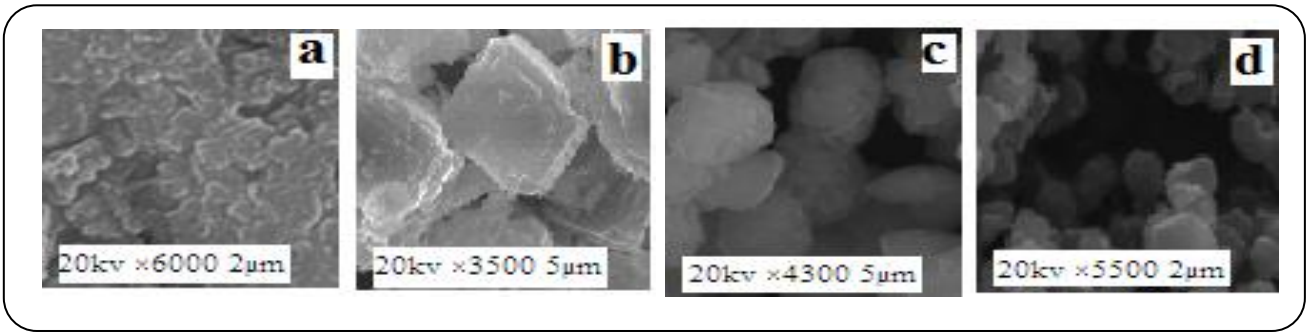

Fig. 5: SEM micrographs of zeolite 13X crystals Produced from metakaolin in different concentrations of NaOH.

the reaction between NaOH and metakaolin, SiO_2 and Al_2O_3 are transformed into aluminosilicates. Their vibration bands in the IR spectrum are replaced by a single band around 1000 cm^{-1}, characteristic of Si–O–Al bonds in TO4 tetrahedral [35].

The appearances of the zeolite produced from metakaolin at various concentrations of NaOH are shown in SEM micrographs (Fig. 5). From these morphological SEM images, the synthesized sample can be seen more clearly. Micropore structure and abundant pores in it, indicate the high adsorption capacity of the sample. According to the experimental results of this work, the data obtained by SEM correlate and agree with the mineralogical composition of the zeolite products, which was determined through XRD results.

N_2 adsorption-desorption isotherm of synthesized zeolite measured with nitrogen gas at 77K presented in Fig. 6. The isotherm of synthesized zeolite showed a typical type I behavior [36]. The low-pressure isotherm provides information about microporosity. To find the highest specific surface area, BET analysis was performed. The surface areas of the metakaolin samples (in Table 1) were calculated using the Brunauer–Emmett–Teller (BET) method. Furthermore, the micropore surface area as well as external surface area and micropore volume are obtained by the t-plot method. The synthesis of zeolite 13X textural properties is listed in Table 4. The synthesis zeolite 13X in this table was obtained from metakaolin and its compositions are given in Table 1. Further information was given in references [2-5, 7-13].

Analysis of Taguchi design of experiment

After performing the experiments, their measured characteristics were used to analyze the relative effect of different parameters. The crystallinity of final products was considered as the quality characteristic and measured response. Analysis of variance (ANOVA) was employed to assess the impact of selected parameters and determine

Table 4: Textural properties of synthesis zeolite 13X from metakaolin (in Table 1) [2].

BET surface area (m^2/g)	Micropore surface area (m^2/g)	Micropore volume (cm^3/g)	External surface area (m^2/g)
591	576	0.250	34

Table 5: Optimum condition and performance for NaX zeolite synthesis.

Parameters	Level Description	Level
Na_2O/ Al_2O_3	4.5	1
SiO_2/Al_2O_3	2.5	1
Temperature (ºC)	65	2
time (h)	72	3

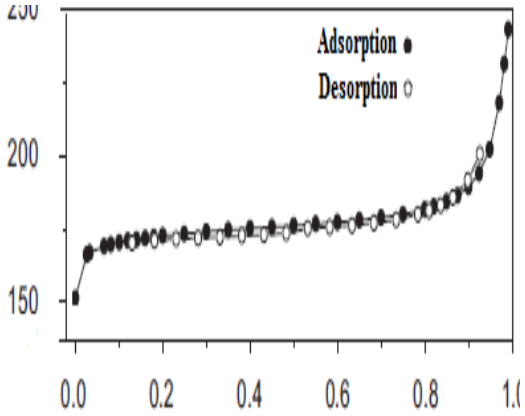

Fig. 6: N_2 adsorption-desorption isotherm [2].

the optimum level of them. Calculation of ANOVA is based on the total and factors sum of squared deviations which are given by the following relations [37]:

The total sum of squares:

$$S_T = \left[\sum_{i=1}^{N}(Y_i)^2\right] - \frac{T^2}{N} \quad (4)$$

Where Y_i is the *i-th* obtained data value, N is the number of observations and T is the total of all observations. Factor sum of square due to parameter A:

$$S_A = \left[\sum_{i=1}^{K_A}\left(\frac{A_i^2}{N_{Ai}}\right)\right] - \frac{T^2}{N} \quad (5)$$

Where K_A is the number of levels for parameter A, A_i^2 is the sum of results (Y_i) where parameter A_i^2 is present, and N_{Ai} number of experiments where *i-th* level of factor A is present. Other given data in the ANOVA table are calculated based on the sum of squares. For each factor they are as follows:

Mean square:

$$V_A = \frac{S_A}{f_A} \quad (6)$$

The pure sum of squares:

$$S'_A = S_A - (V_A \times f_A) \quad (7)$$

Percent influence:

$$P_A = \frac{S'_A}{S_A} \times 100 \quad (8)$$

The optimum conditions for achieving the maximum crystallinity of zeolite 13X are summarized in Table 5.

Fig. 7 indicates the best levels for each factor. Therefore, the optimum conditions for removal of hydrogen sulfide adsorption are as follows: (1) the Na_2O/ Al_2O_3 ratio is 4.5; (2) the SiO_2/Al_2O_3 ratio is 2.5; (3) the best temperature of crystallization is 65ºC; and (4) the suitable duration of crystallization time is 72h.

Isotherms of H_2S adsorption

Adsorption isotherms in optimizing the use of adsorbents are very important and critical [38]. In this work, the CO_2 and CH_4 adsorption data on zeolite 13X at a temperature ranging from 298 K to 318 K were fitted to standard isotherm models. The Langmuir equation is described by the following:

$$q = q_m[bp/(1+bp)] \quad (9)$$

Where b is the affinity constant or Langmuir constant and q_m is a constant that reflects a complete monolayer.

For heterogeneous surface energy systems the Freundlich isotherm is expressed as

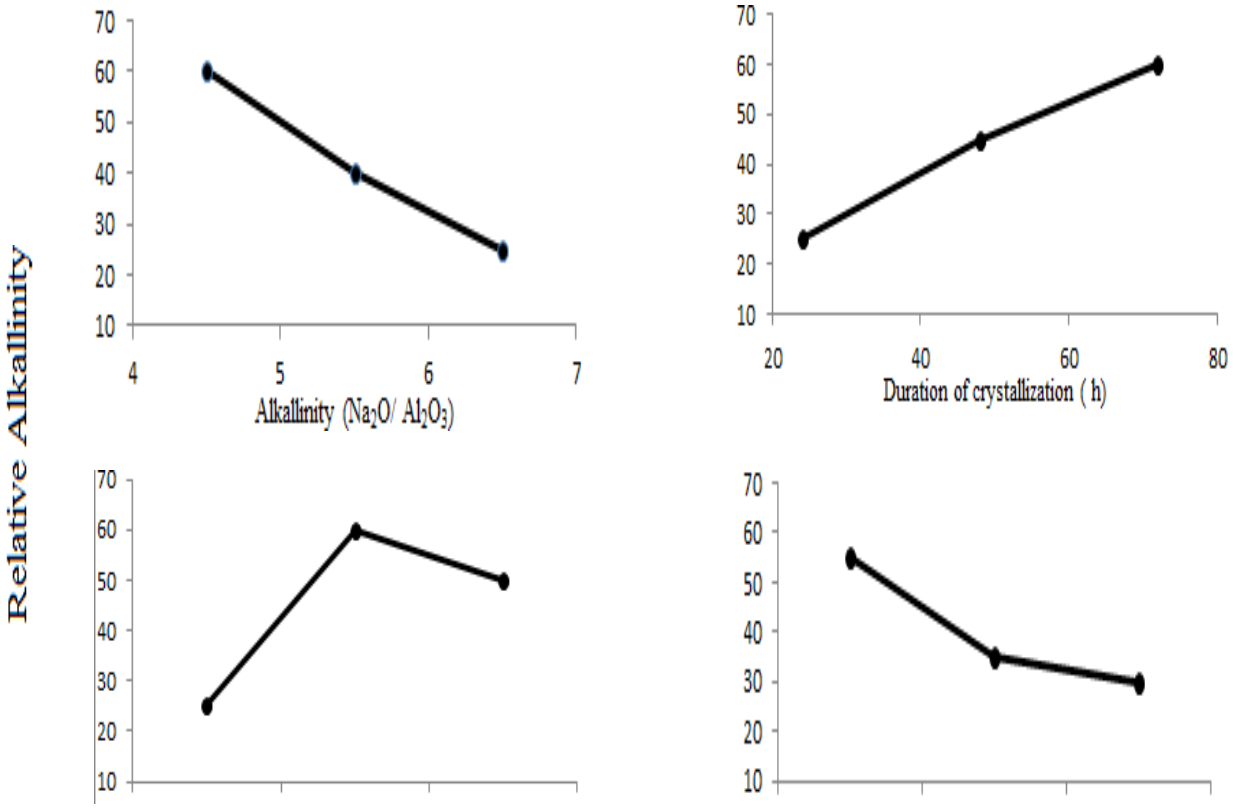

Fig. 7: Effects of controllable factors.

$$q = kp^{1/n} \quad (10)$$

Where k and n are constants for a given adsorpbent-adsorbate system.

The Sips isotherm model can be expressed as

$$q = \frac{q_m (bP)^{1/n}}{1 + (bP)^{1/n}} \quad (11)$$

$$b = b_0 \exp\left[\frac{Q}{RT_0}\left(\frac{T_0}{T} - 1\right)\right] \quad (12)$$

$$\frac{1}{n} = \frac{1}{n_0} + \alpha\left(1 + \frac{T_0}{T}\right) \quad (13)$$

q, is the concentration of the adsorbed phase, q_s is the maximum adsorbed amount, Q is the isosteric heat of adsorption at half loading, b_0 is the adsorption constant at the reference temperature T_0, and n is a parameter that characterizes the solid–fluid interaction. With the system heterogeneity the magnitude of n increases, and when n = 1, the Sips isotherm reduces to the Langmuir isotherm. The parameters n_0 and α describe the temperature dependence of the heterogeneity parameter n.

The Toth isotherm model is given by

$$q = \frac{q_m (bP)}{[1 + (bP)^t]^{1/t}} \quad (14)$$

$$t = t_0 + \alpha\left(1 + \frac{T_0}{T}\right) \quad (15)$$

$1/t$ is similar to the physical meaning of parameter n in the Sips model.

At different pressures in the range 0-25 bar the absolute adsorption isotherm of H_2S on synthesized 13X zeolite at 298 K was examined (Fig. 7). The dashed line refers to measure by Gastec-4H tube detector and the solid line shows the sorption capacity of synthesized zeolite against H_2S using an MSA5Xgas detector. The experiment was done at pressures 5, 10, 15, 20, and 25 bar at ambient temperature (298 k). The simulated gas mixture was contained 99.99% butane and 310 ppm H_2S. The results

Table 6: The parameters of H_2S adsorption isotherms at different temperatures on synthetic zeolite 13X. (SiO_2/Al_2O_3 :2.5 and Na_2O/Al_2O_3 : 2.5 and 4.5 and NaOH:4.0 M.)

Models Equation	Temperatures (K)	parameters					
Langmuir model $q = q_m[bp/(1+bp)]$	298	q_m= (mmol/g× 10^{-4})	204	b= (× 10^{-5})	6.90	R^2=	0.9979
	308		188		6.31		0.9955
	318		170		6.12		0.9940
	328		114		5.48		0.9909
Toth model $q = \frac{q_m(bP)}{[1+(bP)^t]^{1/t}}$	298		168		5.62		0.9624
	308		135		5.41		0.9535
	318		115		5.13		0.9330
	328		93		4.97		0.9330
Sips model $q = \frac{q_m(bP)^{1/n}}{1+(bP)^{1/n}}$	298		185		5.88		0.9812
	308		150		5.62		0.9754
	318		120		5.51		0.9621
	328		98		5.17		0.9501
Freundlich model $q = kp^{1/n}$	298	k=	1.98	n=	1.58		0.9887
	308		1.58		1.22		0.9812
	318		1.44		1.28		0.9714
	328		1.41		1.09		0.9620

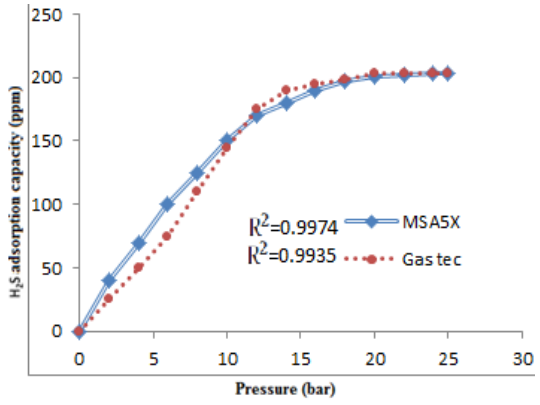

Fig.8: Adsorption equilibrium isotherms of hydrogen sulfide adsorbed on zeolite 13X (The zeolite was synthesized by these ratios: SiO_2/Al_2O_3 :2.5 and Na_2O/Al_2O_3 : 2.5 and 4.5 and NaOH:4.0 M) at different temperatures.

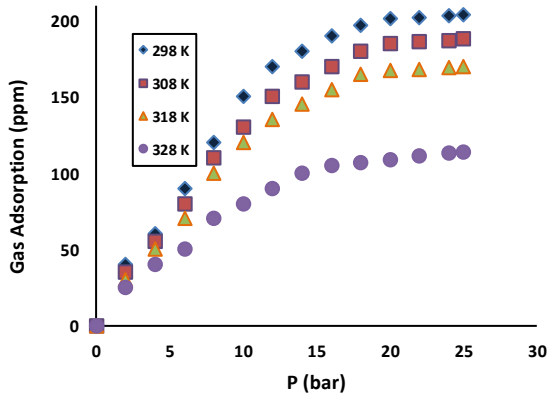

Fig.9: H_2S adsorption isotherm by synthesized 13X zeolite (The zeolite was synthesized by these ratios: SiO_2/Al_2O_3 :2.5 and Na_2O/Al_2O_3 : 2.5 and 4.5 and NaOH:4.0 M.)at different temperatures.

are in good agreement when the Gastec tube detector was used.

Adsorption equilibrium isotherms of hydrogen sulfide adsorbed on zeolite 13X at different temperatures are presented in Fig. 8 and Fig. 9. The zeolite was synthesized by these ratios: SiO_2/Al_2O_3 :2.5 and Na_2O/Al_2O_3 : 2.5 and 4.5 and NaOH:4.0 M. According to the IUPAC classification, all curves can be classified as Type-1.

Moreover, hydrogen sulfide adsorption isotherm parameters at different temperatures on synthesis zeolite 13X show in Table 6. Here, with increasing the temperature, the value of q_m decreased. High values of b are reflected in the steep initial slope of a sorption isotherm, indicating desirable high affinity. Thus, for a good adsorbent in general, high q_m and a steep initial isotherm slope (i.e., high b) is desirable.

Table 7: Gibbs free energy value as a function of the adsorption temperature.

Temperature (K)	ΔG (kJ/mol)
298	-3.14
308	-3.21
318	-3.42
328	-3.71

Table 8: H_2S removal by different zeolites.

Zeolite type	Sulfur reduction	Reference
Commercial 4A	61 %	[39]
Commercial 5A	84-85 %	[39]
Commercial 13X	84-85 %	[39]
LTA	20% after 24h	[40]
Fe-Na-A	0.2-1.5 %	[41]
Na-A	31 %	[42]
H-Y	59 %	[42]
Synthesis 13X	62 %	[20]
Synthesis 13X	65 %	This work

Table 9: Degree of crystallinity DC % determined by various methods [48].

Sample	Amount
Si/Al	1.44
Na/Al	0.97

The positive value of ΔS^0_{ads} in Table 7 shows that the affinity of the adsorbent for CO_2 adsorption, the positive value of ΔH^0_{ads} indicates that the adsorption process is endothermic and the negative values of ΔG^0_{ads} indicate the spontaneous nature of the adsorption of CO_2 on the adsorbent [43-47].

By plotting the isotherm, it is concluded that the quick steep increase monolayer H_2S adsorption at low pressure belongs to type I and follows by the kinetic Langmuir model [20]. Some experimental approaches for pure H_2S removal by zeolites are tabulated in Table 8. *Bandarchian et al.* [20] investigated the adsorption of trace amount of hydrogen sulfide from mixture with propane and uptake of 62% H_2S approach. Removal of pure hydrogen sulfide by commercial 4A, 5A , and 13X zeolite by *Ning et al.* [38-39] was done and had good results. Commercial zeolites synthesis by chemical pure materials that are commonly expensive and limited to use for industrial applications.

The degree of crystallinity of samples was determined by i.r. method ($DC_{i.r}$) [48] which is shown in Table 9. As revealed from this table, the degree of crystallinity of zeolite 13X containing the Si/Al is higher than the others.

CONCLUSIONS

Synthesis of zeolite 13X from modified natural Iranian kaolin, i. e. metakaolin, at 65˚C for 72 h in various concentrations of NaOH solutions is made. Metakaolin was obtained by calcining kaolin in a muffle furnace at 900 ˚C for 2h. Design of experiments was done and due to the results of Taguchi experimental design, the best SiO_2/Al_2O_3 and Na_2O/Al_2O_3 were 2.5 and 4.5.from this design, crystallization duration and temperature were 72h and 65˚C. The zeolite 13X that was produced by this process, was characterized by X-ray diffraction (XRD), Fourier transforms infrared spectroscopy (FTIR), and scanning electron microscopy (SEM), and N_2 adsorption-desorption methods. All results are in good agreement with the literatures. To continue, its adsorption properties for the separation of trace amounts of hydrogen sulfide (in terms of ppm) from Butane gas were investigated in different pressures in the range 0-25 bar based on the volumetric method. The rate of H_2S uptake was directly affected by the pressure of gas passing through the bed. The adsorption capacity of synthesis zeolite 13X at 25 bar and 298 K is found to be about 65%.

Received: Oct. 4, 2021 ; Accepted: Jan. 3, 2022

REFERENCES

[1] Honarmand S., Moosavi E.S., Karimzadeh R., Synthesis of Zeolite Y from Kaolin and Its Model Fuel Desulfurization Performance: Optimized by Box- Behnken Method, *Iran. J. Chem. Chem. Eng. (IJCCE)*, **39(1)**: 79-90 (2020).

[2] Garshasbi V., *Ph.D. Thesis*, "Investigation of Adsorption and Diffusion of Sulfur By Zeolitic Nano Structure Adsorbent", Semnan University, (2018).

[3] Garshasbi V., Jahangiri M., Anbia M., Equilibrium CO_2 Adsorption on Zeolite 13X Prepared from Natural Clays, *Applied Surface Science*, **393:** 225–233 (2017).

[4] Garshasbi V., Jahangiri M., Anbia M., Adsorption of Carbon Dioxide and Methane on Nano-Size Sodalite Octahydrate Zeolite, *Particulate Science and Technology*, **36(6)**: 660-665 (2018).

[5] Pedram T., Eshaghi Z., Ahmadpour A., Nakhaei A., Optimization of Adsorption Parameters Using Central Composite Design for the Removal of Organosulfur in Diesel Fuel by Bentonite-Supported Nanoparticle NiO-WO_3, *Iran. J. Chem. Chem. Eng. (IJCCE)*, **41(3)**: 808-820 (2022).

[6] Sharifi F., Jahangiri M., Ebrahimnejad P., A Novel Efficient MPEG-Chitosan/HA Biopolymer for Adsorption of the Anticancer SN-38 Liquid Dispersions: Kinetics, Thermodynamic and *Ex-Vivo* Release Evaluation, *J. Mex. Chem. Soc.* **65(4)**: 516-534 (2021).

[7] Ma Y., Yan C., Alshameri A., Qiu X., Zhao C., Ii D., Synthesis and Characterization of 13X Zeolite from Low-Grade Natural Kaolin, *Advanced Powder Technology*, **25**: 495-500 (2014).

[8] Chen D., Hu X., Shi L., Cui Q., Wang H.Y., Yao H.Q., Synthesis and Characterization of Zeolite X From Lithium Slag, *Applied Clay Science*, **59**: 148-151 (2012).

[9] Kazemian H., Naghdali Z., KashaniT.G., Farhadi F., Conversion of High Silicon Fly Ash to Na-P1 Zeolite: Alkaline Fusion Followed by Hydrothermal Crystallization, *Advanced Powder Technology*, **21**: 279-284. (2010)

[10] Wajima T., Haga M., Kuzawa K., Ishimoto H., Tamada O., Ito K., Nishiyama T., Downs R.T., Pakovan J.F., Zeolite Synthesis from Paper Sludge Ash at Low Temperature (90 °C) with Addition of Diatomite, *Journal of Hazardous Materials*, **132**: 244-252 (2006).

[11] Pornomo C.W., Salim C., Hinode H., Synthesis of Pure Na–X and Na–A Zeolite from Bagasse Fly Ash, *Microporous and Mesoporous Materials*, **162**: 6-13 (2012).

[12] Eskandari A., Jahangiri M., Anbia M., Effect of Particle Size of NaX Zeolite on Adsorption of CO2/CH4, *International Journal of Engineering, IJE TRANSACTIONS A: Basics*, **29(1)** :1-7 (2016).

[13] Eskandari A., Anbia M, Jahangiri M., Nejati F.M., Investigation of the Use of Various Silica Source on NaX Zeolite Properties, *Journal of Chemical and Petroleum Engineering*, **50(2)**: 1-7 (2017).

[14] Colina F.G, Liorens J., Study of the Dissolution of Dealuminated Kaolin in Synthesis, *Microporous and Mesoporous Materials*, **100:** 302-306 (2007).

[15] Sheibani S., Zare K., Safavi S. M. M., Investigation of Oxidative Desulfurization of Light Naphtha by NiMo/γ-Al2O3 Catalyst, *Iran. J. Chem. Chem. Eng. (IJCCE)*, **40(2)**: 417-427 (2021).

[16] Park J.E., Youn H.K., Yang S.T., Ahn,W.S., CO_2 Capture and MWCNTs Synthesis Using Mesoporous Silica and Zeolite 13X Collectively Prepared from Bottom Ash, *Catalysis Today*, **190**: 15-22 (2012).

[17] Yu L., Gong J., Zeng C., Zhang L., Synthesis of Monodisperse Zeolite A/Chitosan Hybrid Microspheres and Binderless Zeolite A Microsphere, *Industrial & Engineering Chemistry Research*, **51**: 2299-2308 (2012).

[18] Dunne J.A., Rao M., Sircar S., Gorte R.J., Mayers A.L., Calorimetric Heats of Adsorption and Adsorption Isotherms O_2, N_2, Ar, CO_2, CH_4, $C2H_6$ and SF6 on NaX,H-ZSM-5, and Na-ZSM-5 Zeolites, *Langmuir*, **12**: 5896-5904 (1996).

[19] Harlick P.J.E., Tezel F.H., An Experimental Adsorbent Screening Study for CO_2 Removal from N_2, *Microporous and Mesoporous Materials*, **76**: 71-75 (2004).

[20] Bandarchian F., Anbia M., Conventional Hydrothermal Synthesis of Nanoporous Molecular Sieve 13X for Selective Adsorption of Trace Amount of Hydrogen Sulfide from Mixture with Propane, *Journal of Natural Gas Science & Engineering*, **26**: 1380-1387 (2015).

[21] Ozekmekci M., Salkic G.,Fellah, M.F., Use of Zeolites for the Removal of H_2S: A Mini-Review, *Fuel Processing Technology*, *Catalysts*, **139**: 49–60 (2015).

[22] Malek Alaie M., Jahangiri M., Rashidi A.M., Haghighi Asl A., Izadi N., Selective Hydrogen Sulfide (H_2S) sensors Based on Molybdenum Trioxide (MoO_3) Nanoparticle Decorated Reduced Graphene Oxide, *Materials Science in Semiconductor Processing*, **38**: 93–100 (2015).

[23] Malek Alaie M., Jahangiri M., Rashidi A.M., Haghighi Asl A., Izadi N., A Novel Selective H_2S Sensor Using Dodecylamine and Ethylenediamine Functionalized Graphene Oxide, *Journal of Industrial and Engineering Chemistry*, **29**: 97–103 (2015).

[24] Bakhtiari G., Bazmi M., Abdouss M., Royaee S.J., Adsorption and Desorption of Sulfur Compounds by Improved Nano Adsorbent: Optimization Using Response Surface Methodology, *Iran. J. Chem. Chem. Eng. (IJCCE)*, **36(4)**: 69-79 (2017).

[25] Mikhail S., Zaki T., Khalil L., Desulfurization by an Economically Adsorption Technique, *Applied Catalysis A: General*, **227**: 265-278 (2002).

[26] Marjani A., Mechanistic Modeling of Organic Compounds Separation from Water *via* Polymeric Membranes, *Iran. J. Chem. Chem. Eng. (IJCCE)*, **36(6)**: 139-149 (2017).

[27] Karge H., Rask O.J., Hydrogen Sulfide Adsorption on Faujasite-Type Zeolites with Systematically Varied Si-Al Ratios, *Journal of Colloid and Interface Science*, **64**: 522-532 (1978).

[28] Parsafar N., Ghafouri V., Banaei A., Electrochemical Sensing of H2S Gas in Air by Carboxylated Multi-Walled Carbon Nanotubes, *Iran. J. Chem. Chem. Eng.(IJCCE)*, **38(6)**: 53-62 (2019).

[29] Ferino I., Monaci R., Rombi E., Solinas V., Burlamacchi L., Temperature programmed desorption of H_2S from alkali-metal zeolites, *Thermochim Acta*, **99**: 45-55 (1992).

[30] Omrani H., Naser I., Rafiezadeh M., Experimental and Numerical Study of CO_2/CH4 Separation Using SAPO-34/PES Hollow Fiber Membrane, *Iran. J. Chem. Chem. Eng. (IJCCE)*, **40(3)**: 841-852 (2021).

[31] Roy R.K., Hamada M.S., Design of Experiments Using the Taguchi Approach, Wiley, New York. (2001).

[32] Anbia M., Hoseini V., Sheykhi S., Sorption of Methane, Hydrogen and Carbon Dioxide on Metal-Organic Framework, Iron Terephthalate (MOF-235), *J. Industrial and Engineering Chemistry*, **18**:1149-1152 (2012).

[33] Rashidi A., Nouralishahi M.A., Khodadadi A.A., Mortazavi Y., Karimi A., Kashefi K., Modification of Single Wall Carbon Nanotubes (SWNT) for Hydrogen Storage, *International Journal of Hydrogen Energy*, **35**: 9489-9495 (2010).

[34] Wang C.Y., Tsao C.S., Yu M.S., Liao P.Y., Chung T.Y., Wu H.C., Miller M.A., Tzeng Y.R., Hydrogen Storage Measurement, Synthesis and Characterization of Metaleorganic Frameworks Via Bridged Spillover. *Journal of Alloys and Compounds*, **492**: 88-94 (2010).

[35] Gougazeh M., Buhl J.C., Synthesis and Characterization of Zeolite A by Hydrothermal Transformation of Natural Jordanian Kaolin, *Journal of the Association of Arab Universities for Basic and Applied Sciences*, **15**: 35-41 (2013).

[36] Anbia M., Nejati, F.M., Jahangiri M., Eskandari A. Garshasbi V., Optimization of Synthesis Procedure for NaX Zeolite by Taguchi Experimental Design and its Application in CO_2 Adsorption, *Journal of Sciences, Islamic Republic of Iran*, **26**: 213-222 (2015)

[37] Roy R.K., A Primer on the Taguchi Method. John Wiley & Sons, Canada. (1997).

[38] Yu Q.F., Tang X.L., Yi H.H., Ning P., Yang L.P., Yang L.N., Yu L.L., Li H., Equilibrium and Heat of Adsorption of Phosphine on $CaCl_2$–Modified Molecular Sieve, *Asia-Pacific Journal of Chemical Engineering*, **4**: 612–617 (2009).

[39] Ning P., Li F., Yi H., Tang X., Peng J., Li Y., He D., Deng H., Adsorption Equilibrium of Methane and Carbon Dioxide on Microwave-Activated Carbon, *Separation and Purification Technology*, **98**: 321-326 (2012).

[40] Tomadakis M.M., Heck H.H., Jubran M.J., Al-Harthi K., Pressure Swing Adsorption Separation of H_2S from CO_2 with Molecular Sieves 4A, 5A and 13X, *Separation Science and Technology*, **46**: 428–433 (2011).

[41] Yokogawa Y., Sakanishi M., Morikawa N., Nakaruma A., Kishida I., Varma H.K., VSC Adsorptive Properties in Ion Exchanged Zeolite Materials in Gaseous and Aqueous Medium, *Procedia Engineering*, **36**: 168–172 (2012).

[42] Lee S.K., Jang Y.N., Bae I.K., Chae S.C., Ryu K.W., Kim J.K., Adsorption of Toxic Gases Iron-Incorporated Na-A Zeolites Synthesized from Melting Slag, *Materials Transactions*, **50**:2476–2483 (2009).

[43] Ali V.K., Suhas I., Mohan D., Equilibrium Uptake and Sorption Dynamics For The Removal of a Basic Dye (Basic Red) Using Low-Cost Adsorbents. *Journal of Colloid and Interface Science*, **265**: 257–264 (2003).

[44] Namasivayam C., Kavitha D., Removal of Congo Red from Water by Adsorption onto Activated Carbon Prepared From Coir Pith, An Agricultural Solid Waste, *Dyes and Pigments*, **54**: 47–58 (2002).

[45] Tan I.A.W., Ahmad A.L., Hameed B.H., Adsorption of Basic Dye on High-Surface-Area Activated Carbon Prepared from Coconut Husk: Equilibrium, Kinetic and Thermodynamic Studies, *Journal of Hazardous Materials*, **154**: 337–346 (2008).

[46] Monier M., Abdel-Latif D.A., Preparation of Cross-Linked Magnetic Chitosan-Phenylthiourea Resin for Adsorption of Hg(II), Cd(II) and Zn(II) Ions from Aqueous Solutions, *Journal of Hazardous Materials*, **209–210**: 240–249 (2012).

[47] Zou W, Han R., Chen Z., Jinghua Z., Shi J., Kinetic Study Of Adsorption of Cu(II) and Pb(II) from Aqueous Solutions Using Manganese Oxide Coated Zeolite in Batch Mode, *Colloids and Surfaces A: Physicochemical and Engineering Aspects*, **279**: 238–246 (2006).

[48] Adnadjevic B., Vukicevic J., Rojka Z.F., Markovc V., The Influence of NaX Zeolite Particle Size on Crystallinity Measured by the XRD Method, *Zeolites*, **10**: 699-702 (1990).